JACS
JOURNAL OF THE AMERICAN CHEMICAL SOCIETY

Communication

pubs.acs.org/JACS

Observation of Exceptionally Low-Lying $\pi-\pi^*$ Excited States in Oxidized Forms of Quadruple-Decker Phthalocyanine Complexes

Takamitsu Fukuda,* Kentaro Hata, and Naoto Ishikawa*

Department of Chemistry, Graduate School of Science, Osaka University, Toyonaka, Osaka 560-0043, Japan

Supporting Information

ABSTRACT: Spectroscopic investigations have been performed for the oxidized forms of two quadruple-decker phthalocyanine complexes in order to clarify the electronic structures of multiply stacked π-systems. Up to three-electron-oxidized species were isolated by using phenoxathiin hexachloroantimonate as the oxidant. As the oxidations proceed, the Q-bands in the visible region shift bathochromically along with the clear isosbestic points. The one- and three-electron-oxidized species exhibited typical π-radical signals in the ESR spectra, while the neutral and two-electron oxidized species gave no indication of the presence of π-radicals. The electronic transitions observed for the oxidized species reach even into the so-called fingerprint region in IR spectroscopy ($\sim$1000 cm^{-1}). With the aid of theoretical calculations, these bands can be assigned to the $\pi-\pi^*$ transitions. Our results provide new insights into π-electronic systems having exceptionally small MO energy gaps.

A variety of π-conjugated molecules such as polyacene, cyclophane, porphyrin, fullerene, and graphene analogues have been designed and synthesized in recent decades. Versatile physicochemical properties arising from the unique π-electronic structures of these molecules have been substantiated, giving us an in-depth understanding of the electronic structures of π-conjugated molecules.[1] In particular, the loosely bound nature of π-electrons compared to σ-electrons often results in the observation of $\pi-\pi^*$ excited states in the visible to near-infrared (NIR) region, due to closely lying molecular orbitals (MOs). Engineering π-electronic systems with narrow energy gaps has been a key to realizing leading-edge optoelectronic molecular devices such as unprecedented photoconductive, infrared-electrochromic, and charge-storage molecular materials.[2] In most cases, molecules having higher degrees of π-conjugation exhibit lower excitation energies, as simply demonstrated in the electronic absorption spectra of benzene, naphthalene, and anthracene.[3] These bathochromic effects are attributed mainly to either destabilization of the HOMO or stabilization of the LUMO of the molecule in order to achieve the smaller energy gap between the occupied and unoccupied frontier MOs.[2] The π-conjugated molecules exhibiting lower $\pi-\pi^*$ excitation energies have been realized with these "extension approaches", in which the π-components are arranged linearly or two-dimensionally, maintaining conjugation over the molecule.[1d,4] A series of fully conjugated porphyrin tapes are renowned examples of linearly expanded π-molecules.[5] The UV–vis spectra of graphitic discs with different sizes exhibit lower-energy absorption bands (α-bands) with increasing number of conjugated six-membered rings.[1d] As an alternative strategy for expanding the π-conjugations, longitudinal stacking of the components is also attractive, although information on electronic structures in this type of molecules is limited to date due to synthetic difficulties. The simple MO model predicts that the energy differences between the occupied frontier orbitals become smaller with increasing number of stacked aromatic units, leading to a continuous band structure in the ideal infinite chain limit. On the other hand, molecules in which multiple numbers of π-conjugated units are stacked longitudinally are anticipated to exhibit electronic structures defined as intermediate between discrete molecules and bulk solids.

Phthalocyanine (Pc) ligands have been known to form doubly or triply stacked conformations to yield the so-called double- or triple-decker complexes when large metal ions such as lanthanide(III) ions (Ln^{3+}) are employed to connect the two or three Pc ligands in a longitudinal fashion. Recently, the first discrete quadruple-decker Pc complex was synthesized by Fukuda et al. by reaction of two double-decker Pc's with a cadmium(II) ion,[6] which opened the way to general procedures for synthesizing multiple-decker Pc complexes.[7] Since the HOMO of the Pc monomer is energetically isolated from the HOMO−1 and LUMO, the occupied frontier MOs of the stacked Pc's can be approximated by linear combinations of the HOMOs of the constituent units. For the double- and triple-decker Pc complexes, indeed, the one-electron-oxidized forms of these complexes, i.e. $[Ln^{III}Pc(2-)_2]^0$ and $[Ln^{III}{}_2Pc(2-)_3]^+$, exhibit absorption bands at $\sim$7000 and 4600 cm^{-1} ($\sim$1400 and 2200 nm), respectively, indicating that the increased number of Pc ligands shifts the lowest electronic transitions to the lower-energy region.[8]

In the present study, quadruple-decker Pc's **2a** and **2b** (Scheme 1) have been prepared, and the spectroscopic properties of the oxidized forms of these molecules are elucidated in order to clarify how the occupied frontier MOs are affected by the stacked molecular arrangements. The experimental results with the aid of theoretical calculations successfully demonstrate that the oxidized forms of the quadruple-decker Pc's exhibit $\pi-\pi^*$ transitions in the exceptionally low energy region.

2a and **2b** were synthesized according to our original methods with some modifications on the purification

Received: July 3, 2012
Published: August 28, 2012

   dx.doi.org/10.1021/ja3064606 | J. Am. Chem. Soc. 2012, 134, 14698–14701

Scheme 1. Synthesis of Quadruple-Decker Phthalocyanines 2a and 2b

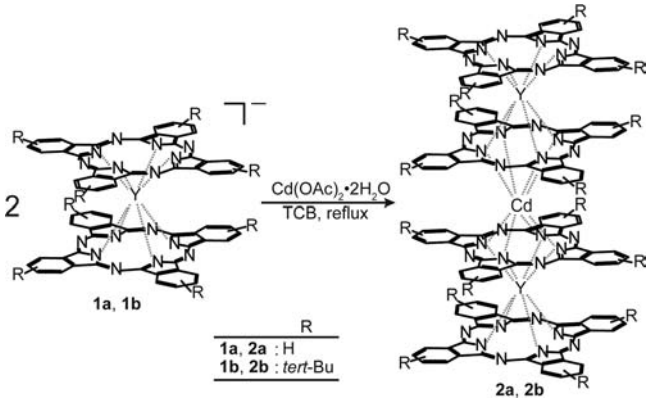

procedures.[6,7a] Yttrium complexes of the double-decker Pc's, **1a** and **1b**, were reacted with cadmium acetate in refluxing trichlorobenzene to give the corresponding quadruple-decker **2a** and **2b** in 2.3 and 6.6% yield, respectively. Since the poor solubility of the unsubstituted derivative **2a** prevents a detailed spectroscopic study of the oxidized species, the highly soluble *tert*-butyl-substituted derivative **2b** was used to collect supplemental data.

Figure 1 displays the cyclic voltammograms of **2a** and **2b**, with redox potential data given in Table 1. At least three

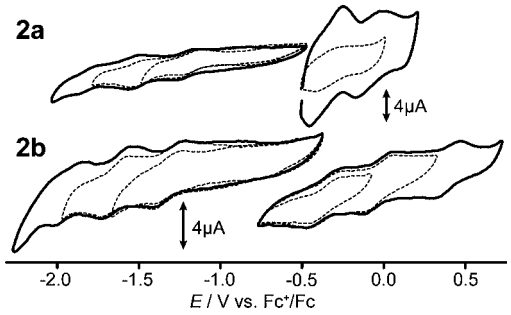

Figure 1. Cyclic voltammograms of **2a** and **2b** in *o*-DCB containing 0.1 M tetrabutylammonium perchlorate. Sweep rate = 20 mV/s.

Table 1. Redox Potentials (V) vs Fc^+/Fc in *o*-DCB

compd	3rd red.	2nd red.	1st red.	1st ox.	2nd ox.	3rd ox.
2a	−1.82	−1.54	−1.25	−0.36	−0.09	
2b	−1.94	−1.65	−1.34	−0.36	−0.04	0.39

reversible reduction steps are observed for both complexes. Compared to unsubstituted **2a**, the reduction potentials of **2b** are shifted to the negative by 0.09−0.12 V, due to the moderate electron-donating nature of the peripheral *tert*-butyl groups. Compound **2b** exhibits three oxidation processes, while only two clear oxidation steps were observed for **2a** at the applied sweep rate, indicating that the oxidized quadruple-decker species tend to aggregate unless the appropriate substituents are present. Although the electrochemical results indicate that the *tert*-butyl groups have some effect on the redox potentials of the quadruple-deckers, they are less significant for the electronic structures of the π-conjugated systems.

Development of the visible region absorption spectra during the chemical oxidation of **2b** using phenoxathiin hexachloroantimonate as oxidant is shown in Figure 2. Unsubstituted **2a** shows spectral changes practically identical with those of **2b** during the oxidations, although low solubilities of the oxidized forms of **2a** required an optical cell path length of 10 cm (see SI). Neutral **2b** exhibits two distinct absorption bands at ∼15 850 and 13 810 cm^{-1} (630 and 724 nm). Upon addition of the oxidant, these Q-band components lose their intensity; instead, a single Q-component appears at 15 190 cm^{-1} (660 nm) along with isosbestic points at 14 210, 15 440, and 17 790 cm^{-1}. Growth of a broad band is also observed at ∼20 000 cm^{-1}. The second oxidation step to yield $\mathbf{2b}^{2+}$ was observed also spectroscopically upon further addition of the oxidant. The Q-component shifts to 14 680 cm^{-1} (680 nm). The broad band at ∼20 000 cm^{-1} gains additional intensity, as depicted in Figure 2 (middle). The third oxidation step proceeds along with the four isosbestic points at 13 400, 14 230, 17 400, and 19 360 cm^{-1}, resulting in the Q-component at 14 030 cm^{-1} (713 nm). The broad band in the 18 000−21 000 cm^{-1} region is shifted slightly to the lower-energy side during this process.

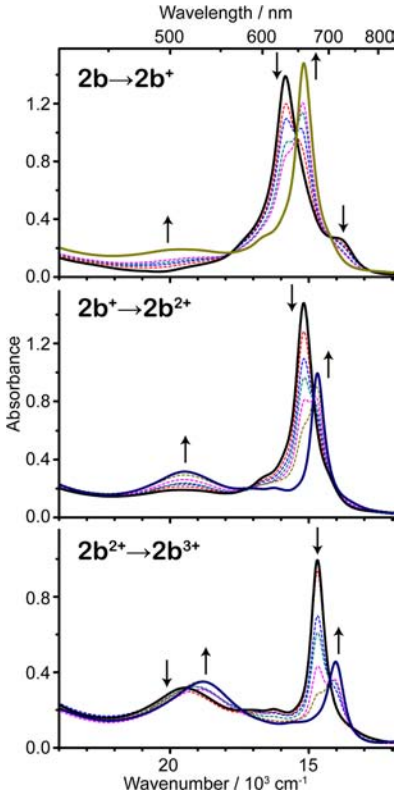

Figure 2. Development of UV−vis absorption spectra in the course of $\mathbf{2b}\rightarrow\mathbf{2b}^{+}$ (top), $\mathbf{2b}^{+}\rightarrow\mathbf{2b}^{2+}$ (middle), and $\mathbf{2b}^{2+}\rightarrow\mathbf{2b}^{3+}$ (bottom) oxidation steps in CH_2Cl_2. Cell path length = 1 cm.

The oxidation processes were also monitored by ESR spectroscopy (see SI). The initial neutral **2b** was ESR silent, while a clear derivative-shaped signal with g = 2.0020 was recorded for the first oxidation product, i.e. $\mathbf{2b}^{+}$, indicating that the π-radical is generated by the first oxidation process. After completion of the second oxidation step to yield $\mathbf{2b}^{2+}$, the ESR signal becomes flat again, suggesting that the two electrons of the original HOMO are removed by the two-step oxidation processes to give the singlet species. Further addition of the oxidant to give $\mathbf{2b}^{3+}$ regenerated the ESR signal with g = 2.0022 due to the presence of the π-radical. The observation of isosbestic points in the absorption spectra and the on−off

dx.doi.org/10.1021/ja3064606 | J. Am. Chem. Soc. 2012, 134, 14698−14701

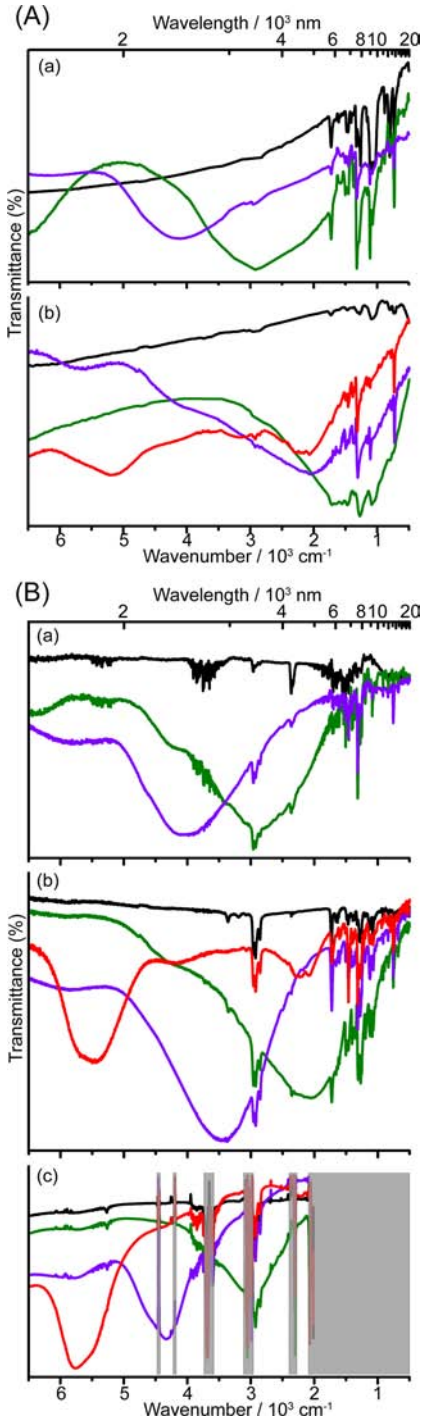

Figure 3. Electronic transitions of (A) unsubstituted and (B) *tert*-butyl-substituted quadruple-deckers observed in the NIR-to-IR energy region. The neutral and one-, two-, and three-electron-oxidized species are represented by black, green, purple, and red lines, respectively. The spectra were obtained by using (a) KBr discs, (b) cast films prepared on KBr crystals, and (c) CH_2Cl_2 solutions in a quartz cell with optical path length of 1 mm. Note that the signals from the CH_2Cl_2 and quartz are masked by the gray shadings in (c).

switching of the ESR signals clearly indicate that each oxidation product can be isolated by careful addition of the oxidant.

The isolated oxidized species were subject to FTIR spectroscopic measurements. Data obtained using KBr pellets, cast films on KBr crystals, and CH_2Cl_2 solutions are depicted in Figure 3A for **2a** and Figure 3B for **2b**. Due to poor solubility, solution spectra could not be obtained for unsubstituted **2a**. In addition, the spectrum of $\mathbf{2a}^{3+}$ in KBr is not presented in Figure 3, because $\mathbf{2a}^{3+}$ rapidly returned to $\mathbf{2a}^{2+}$ during the preparation of the KBr pellets. The neutral species show typical IR spectral envelopes with sharp vibrational signals mainly in the 3000–400 cm^{-1} region (black lines). In contrast, $\mathbf{2b}^{+}$ exhibits a broad signal at 3000 cm^{-1} in CH_2Cl_2 (Figure 3B-(c), green line), which is energetically overlapped with the C–H stretching modes of the *tert*-butyl groups (~2900 cm^{-1}). The corresponding bands appear in similar energy regions for the KBr pellets also, while a further bathochromic shift of the band to ~2000 cm^{-1} is observed for the sample deposited on the KBr crystals (Figure 3B-(b)). Interestingly, the lowest-energy band reaches ~1000 cm^{-1} for the unsubstituted $\mathbf{2a}^{+}$ deposited on KBr crystals (Figure 3A-(b), green line). It is conjectured that the spectra observed in CH_2Cl_2 best reflect the spectroscopic properties of the isolated molecules, because the largest intermolecular distances are expected in the solution phase. While the samples are diluted also in the KBr pellets, significant intermolecular interactions cannot be avoided for the cast films. Comparison of parts A and B of Figure 3 suggests that the presence of the bulky *tert*-butyl groups inhibits these intermolecular interactions to some degree. For the two-electron-oxidized species $\mathbf{2a}^{2+}$ and $\mathbf{2b}^{2+}$, the lowest band shifts to the higher-energy side by ~1500 cm^{-1} (purple lines). In the case of $\mathbf{2b}^{3+}$, the band splits into two components to give a relatively intense signal at ~5700 cm^{-1} and a less intense component at ~2000 cm^{-1} (red lines).

To rationalize the observed spectra, (TD)DFT calculations were performed for a series of oxidized species of **2a**. Energy diagrams for selected MOs are depicted in Figure 4, with selected excitation energies and related wavefunctions in Table 2 and MO amplitudes of the neutral species summarized in Figure 5.

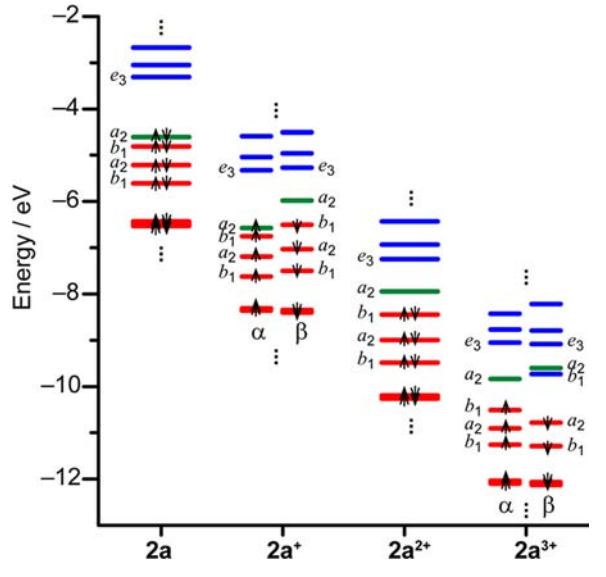

Figure 4. Partial MO energy diagrams of **2a** and its oxidized species predicted by DFT calculations using the B3LYP functional with the LanL2DZ basis set. The |545⟩ wavefunctions corresponding to the HOMO of neutral **2a** are represented by the green bars. The other occupied and unoccupied orbitals are depicted by red and blue bars, respectively. Unrestricted calculations were performed for the one- ($\mathbf{2a}^{+}$) and three-electron-oxidized ($\mathbf{2a}^{3+}$) radical species.

dx.doi.org/10.1021/ja3064606 | J. Am. Chem. Soc. 2012, 134, 14698–14701

Table 2. Calculated Electronic Excitation Energies (E), Oscillator Strength (f), and Related Wavefunctions

compd	E (cm^{-1})	E (nm)	f	wavefunction[a]
$\mathbf{2a}^{+}$	3060	3263	0.18	$1.05\|545\beta\leftarrow544\beta\rangle + \cdots$
$\mathbf{2a}^{2+}$	4630	2160	0.35	$0.82\|545\leftarrow544\rangle + \cdots$
$\mathbf{2a}^{3+}$	3060	3269	0.058	$0.92\|545\alpha\leftarrow544\alpha\rangle + 0.42\|544\beta\leftarrow543\beta\rangle + \cdots$
	5800	1725	0.26	$0.83\|544\beta\leftarrow543\beta\rangle - 0.43\|545\alpha\leftarrow544\alpha\rangle - 0.35\|545\alpha\leftarrow542\alpha\rangle - 0.18\|545\beta\leftarrow542\beta\rangle \cdots$

[a]Note that $|545\rangle$ and $|544\rangle$ correspond to the HOMO and HOMO−1 of the neutral species **2a**, respectively. The α and β notations in the wavefunctions indicate the transitions within the α and β orbitals obtained from the unrestricted calculations. The original unnormalized outputs from the Gaussian software are shown as the wavefunctions.

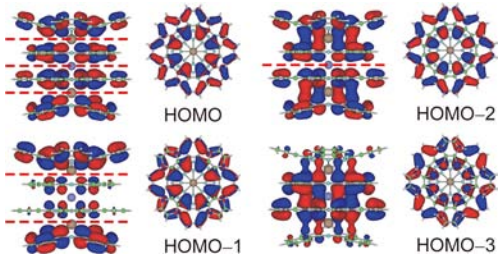

Figure 5. Side (left) and top (right) views of occupied frontier MO amplitudes of **2a**. Nodes between neighboring Pc ligands are indicated by red dashed lines.

Unrestricted calculations were employed for radical species $\mathbf{2a}^{+}$ and $\mathbf{2a}^{3+}$, in which the molecules are assumed to have one additional α electron. The neutral **2a** has no transitions in the NIR-IR region (not shown). On the other hand, the lowest allowed transitions are predicted around 3060 cm^{-1} for $\mathbf{2a}^{+}$, which mainly has the $|545\beta\leftarrow544\beta\rangle$ ($a_2\leftarrow b_1$) one-electron transition at its origin. Therefore, the band observed at 3000 cm^{-1} (Figure 3) can be assigned to $\pi-\pi^*$ transition between the highest occupied and lowest unoccupied MOs generated by one-electron oxidation. In other words, the presence of the energetically close occupied frontier MOs of the quadruple-decker Pc's is unambiguously confirmed by observing the transition bands in the IR region. The $a_2\leftarrow b_1$ transition for $\mathbf{2a}^{2+}$ is calculated at 4630 cm^{-1}, consistent with the experimental results. In the case of $\mathbf{2a}^{3+}$, two transitions originating within the α and β orbitals are expected from Figure 4, while the $a_2\leftarrow a_2$ transitions in the β orbitals are symmetry forbidden; indeed, the experimental results clearly demonstrate the presence of two transitions in the NIR-IR spectral region. Figure 5 shows that the HOMO, HOMO−1, HOMO−2, and HOMO−3 of the quadruple-decker have three, two, one, and zero nodes between the Pc monomer units, respectively, indicating that these MOs can be represented basically as linear combinations of the HOMOs of the Pc monomers. Each Pc unit is approximately staggered with respect to the neighboring Pc's in the quadruple-deckers. Appropriate Pc−Pc distances in the quadruple-deckers make possible MO−MO interactions between the neighboring Pc moieties through the MO amplitudes located at the pyrrole α-carbons, yielding consolidated conjugation through the molecules.

In summary, a series of oxidized forms of quadruple-decker Pc complexes, in which two double-decker Pc complexes are connected by a cadmium ion, have been prepared and isolated using phenoxathiin hexachloroantimonate as the oxidant. Spectroscopic investigations reveal that these oxidized species exhibit broad absorption bands in the NIR-IR, which can be assigned to $\pi-\pi^*$ transitions within the original HOMOs of the constituent monomer Pc units. The transition energies reach as low as 1000 cm^{-1} (Figure 3A-b), which, to the best of our knowledge, is the lowest-energy band reported for fully characterized $\pi-\pi^*$ transitions. Our results indicate that the frontier MOs of the longitudinally stacked Pc analogues are energetically closely distributed, giving intermediate electronic states that can be defined somewhere between discrete molecules and bulk solids. We expect that the observations presented here will give new insight in the fields of molecular electronics and material science, in terms of the effect of photophysical properties of molecules on their electronic functions. Spectroscopic elucidations for larger congeners of stacked Pc complexes are in progress.

■ ASSOCIATED CONTENT

Ⓢ Supporting Information

Experimental details, characterization data, and supplemental spectroscopic data. This material is available free of charge via the Internet at http://pubs.acs.org.

■ AUTHOR INFORMATION

Corresponding Author

tfukuda@chem.sci.osaka-u.ac.jp; iskw@chem.sci.osaka-u.ac.jp

Notes

The authors declare no competing financial interest.

■ ACKNOWLEDGMENTS

This work was supported by a Grant-in-Aid For Scientific Research (C) (no. 22550052, T.F.) from Japan Society for the Promotion of Science (JSPS). We thank Mr. Mitsuo Ohama for his help with IR spectroscopy.

■ REFERENCES

(1) (a) Gleiter, R., Hopf, H., Eds. *Modern Cyclophane Chemistry*; Wiley-VCH: Weinheim, Germany, 2004. (b) Kadish, K. M., Smith, K. M., Guilard, R., Eds. *Handbook of Porphyrin Science*, Vols. *1*−*15*; World Scientific: Singapore, 2010−2011. (c) Kadish, K. M., Ruoff, R. S., Eds. *Fullerenes: Chemistry, Physics, and Technology*; Wiley-Interscience: New York, 2000. (d) Wu, J.; Pisula, W.; Müllen, K. *Chem. Rev.* **2007**, *107*, 718.

(2) Perepichka, D. F.; Bryce, M. R. *Angew. Chem., Int. Ed.* **2005**, *44*, 5370.

(3) Perkampus, H. H. *UV-Vis Atlas of Organic Compounds*; Wiley-VCH: New York, 1992.

(4) Watson, M. D.; Fechtenkötter, A.; Müllen, K. *Chem. Rev.* **2001**, *101*, 1267.

(5) Tsuda, A.; Osuka, A. *Science* **2001**, *293*, 79.

(6) Fukuda, T.; Biyajima, T.; Kobayashi, N. *J. Am. Chem. Soc.* **2010**, *132*, 6278.

(7) (a) Fukuda, T.; Kuroda, W.; Ishikawa, N. *Chem. Commun.* **2011**, *47*, 11686. (b) Wang, H.; Quian, K.; Wang, K.; Bian, Y.; Jiang, J.; Gao, S. *Chem. Commun.* **2011**, *47*, 9624. (c) Wang, H.; Kobayashi, N.; Jiang, J. *Chem.—Eur. J.* **2012**, *18*, 1047.

(8) (a) Ishikawa, N. *J. Porphyrins Phthalocyanines* **2001**, *5*, 87. (b) Ishikawa, N.; Okubo, T.; Kaizu, Y. *Inorg. Chem.* **1999**, *38*, 3173.